JOURNAL OF Materials CHEMISTRY

Methane combustion activity of alumina supported Pt, Pd, and Rh catalysts modified by high-energy ion beam irradiation

M. Machida,*[a] H. Taniguchi,[a] T. Kijima[a] and J. Nakatani[b]

[a]*Department of Materials Science, Miyazaki University, 1-1 Gakuen-kibanadai-nishi, Miyazaki 889-21, Japan*

[b]*Chemicals Research Laboratories, Toray Ind. Inc., Nagoya 455, Japan*

100 keV O^+ or N^+ ion implantation was used to study the irradiation effect on the methane combustion activity of 1 mass% Pd, Pt, and Rh supported on γ-Al_2O_3. The catalytic activity of both Pt/Al_2O_3 and Rh/Al_2O_3 was enhanced by the implantation, probably due to the improved dispersion of noble metals. On the other hand, the activity of Pd/Al_2O_3 decreased substantially with an increased dose amount of O^+ or N^+. The Pd $3d_{5/2}$ XPS measurement demonstrated that the as-prepared catalyst contains PdO, which is reduced to Pd metal with increasing ion implantation. This irradiation-induced reaction process also resulted in not only a significant increase of the Pd particle size from 3 to 20 nm, but also a phase transformation of γ- to α-Al_2O_3 after implanting O^+ of 7.5×10^{18} ion g^{-1}.

Introduction

Modification of materials by high-energy ion beam processes is a new and powerful technology for the preparation of functional solid materials with well controlled surface structures and chemical compositions.[1,2] The ion beam processing includes several different phenomena, such as ion implantation, ion beam mixing, sputtering of surface atoms, and physicochemical reactions during the process of the ion beam penetration into the solids. In particular, ion implantation, which incorporates dopant profiles into the surface region, has proven to be a useful tool for the industrial production and modification of semiconductor materials during the last two decades.[2] However, several recent studies have been directed to not only semiconductor device fabrication, but also textured surfaces, such as hard TiN protective coatings,[3] preparation of bio-ceramics,[4] modification of polymers,[5] or high-T_c superconductors.[6] From the economical view point, however, ion implantation does not seem to be widely applied for materials which require a high dosage process.

One of the novel and potential applications of ion implantation must be the preparation of solid catalysts, because catalysis is a totally surface phenomenon which is strongly influenced by surface properties. For instance, supported noble metals are ranked among the most active catalysts for combustion of hydrocarbons. Numerous studies were undertaken to enhance their catalytic activity by use of additives, or by the choice of preparation procedures and support materials.[7] In contrast to these 'chemical' modifications, ion beam irradiation has the advantage of controlling the magnitude its effect by selecting the type of ions, dose, and accelerating energy. Because of the strong beam–solid interactions, ion bombardment is expected to lead to significant structural, topographical, and compositional changes. Structural changes include crystalline–amorphous or amorphous–crystalline conversion, or randomization of ordered structure. Surface topographic change can be seen as the break-up of surfaces, which results in faceting, ripples, or grain boundary deformation.[1,2] Also, ion implantation and sputtering of certain atoms induce compositional changes near the surface. In spite of these promising alterations of near-surface properties, applications of ion implantation to solid catalysts have not been examined so far.

In this study, our primary interest was evaluating the effect of ion implantation on the catalytic properties of the supported noble metal catalysts, Pd/Al_2O_3, Rh/Al_2O_3, and Pt/Al_2O_3. The effect on the catalytic properties is discussed from methane combustion measurements conducted in a conventional flow reactor, together with the results of structural (XRD), microstructural (TEM) and electron spectrometric (XPS) analyses. These experiments suggest the feasibility of the surface modification of catalytic materials with the help of ion beams.

Experimental

Catalyst preparation

Pd, Pt or Rh (1 mass%) was deposited on γ-alumina (JRC ALO-4, surface area, 186 $m^2\ g^{-1}$) by impregnation of palladium(II) nitrate (99%, Wako Pure Chemical Ind. Ltd.), hydrogen hexachloroplatinate(IV) (99.9%, Wako), or rhodium(III) chloride trihydrate (99.5%, Wako), respectively, followed by calcination at 500 °C for 5 h in an air flow. Ion beam irradiation treatment of as-calcined catalysts was performed by a 200 keV ion implanter (Nissin Denki, Co. Ltd.) at the Ion Engineering Center Co. Ltd., Osaka, Japan. As Fig. 1 illustrates, this ion implanter is constructed with a conventional Freeman type ion source, magnetic mass filters, an accelerated beam line, beam deflecting optics and a special vacuum chamber designed for powder samples. The ion beam was focused on the upper surface of a catalyst powder poured into a stainless steel crucible, which can be vibrated supersonically for homogeneous implantation. The continuous irradiation of 100 keV O^+ or N^+ ions was conducted up to certain implant doses. The beam current fluxes of these ion beams were maintained at 10–110 mA, corresponding to the average dose rate, *ca.* 4×10^{11} ion $cm^{-2}\ s^{-1}$. In this paper, the implant dose is expressed in terms of ion g^{-1}, *i.e.*, the number of the implant ions per gram of catalyst powder.

Catalytic reaction and characterization

The samples before and after ion implantation were submitted to catalytic reaction and several characterizations. Catalytic combustion of methane over supported catalysts was examined in a conventional flow reactor at atmospheric pressure. Catalysts (10–20 mesh, 0.20 g) were fixed in a quartz tube by quartz wool at both ends of the catalyst bed. A gaseous mixture of CH_4 (2 vol%) and air (balance) was supplied at $W/F = 0.002$ (g cat) min cm^{-3}. The methane conversion to carbon dioxide in the effluent gas was analyzed by on-line gas chromatography (TCD) with Porapak-Q and molecular sieve

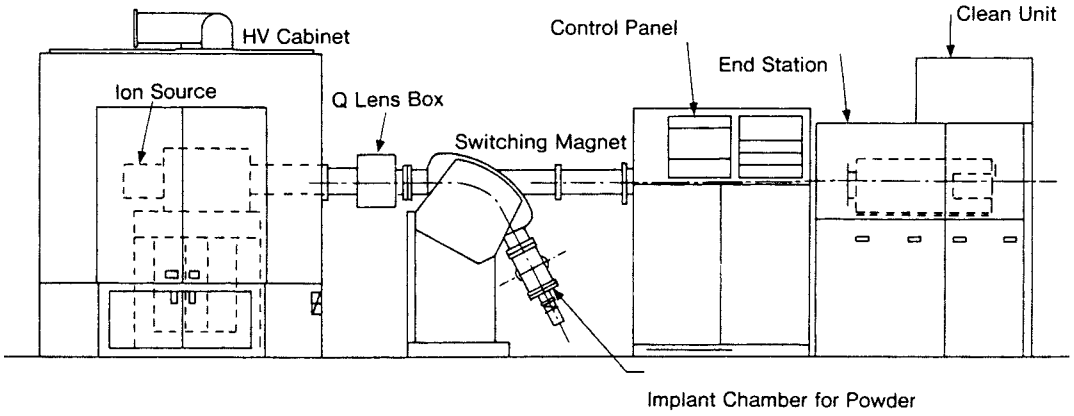

Fig. 1 Schematic illustration of an ion implanter for powder samples

5A columns. The steady state methane conversion was recorded as a function of temperature at the catalyst bed.

Specific surface areas of supported catalysts were determined by the BET method using nitrogen adsorption at 77 K. Surface areas and dispersions of noble metals were evaluated by measuring adsorption isotherms of irreversibly adsorbed H_2 at room temperature. The crystal structure of the catalyst was determined by powder X-ray diffraction (XRD, Rigaku RINT-1400) using Cu-Kα radiation (30 kV; 20 mA). The XPS measurements were performed on a Perkin-Elmer 5600ci spectrometer using Al-Kα radiation (14 kV; 25 mA) at a constant analyzer pass energy of 23.50 eV. The binding energy (E_B) calibration was checked by using the line position of C 1s as an internal reference. The charging effect could be ruled out in these measurements since the E_B for C 1s was identical for all the samples. The normal operating pressure in the analysis chamber was controlled at less than 10^{-6} Pa during the measurements. Transmission electron microscopy (TEM, JEOL 2000FX) was used to observe the microstructures of the catalysts.

Results and Discussion

Methane combustion activity of ion-implanted catalysts

The steady-state CH_4 conversions over Pd/Al_2O_3, Pt/Al_2O_3, and Rh/Al_2O_3 catalysts are shown in Fig. 2 as a function of the reaction temperature. The steady-state product concentration was attained within 30 min at each reaction temperature for all these catalysts before and after ion implantation treatment. Carbon dioxide and water were produced without formation of carbon monoxide in a whole temperature range. The methane combustion activity of the as-prepared catalysts decreases in the order Pd(onset temperature, 240 °C) > Rh(350 °C) > Pt(440 °C), as was already observed by several researchers.[8–10] Although the catalytic activity of Pd was the highest among these catalysts, the complete conversion required rather high temperature (*ca.* 385 °C) as a result of levelling off at > 300 °C.

The ion implantation showed significant effects on the methane combustion activity in different ways. The activity of supported Pt and Rh catalysts was enhanced by the O^+ or N^+ implantation. For instance, the reaction onset of Pt/Al_2O_3 decreased from 440 to 390 °C after N^+ implantation of 14.0×10^{18} ion g^{-1}. Since the methane conversion also tends to increase with increasing implant dose (O^+), the ion implantation produces a positive effect on the catalytic activity of supported Rh and Pt. In contrast, the activity of Pd/Al_2O_3 decreased with an increased dose of O^+ or N^+ (Fig. 2). In this case, N^+ implantation of 14.0×10^{18} ion g^{-1} led to an increased reaction onset from 240 to 280 °C, but much more significant deterioration was observed at high conversion levels ($\geqslant$50%).

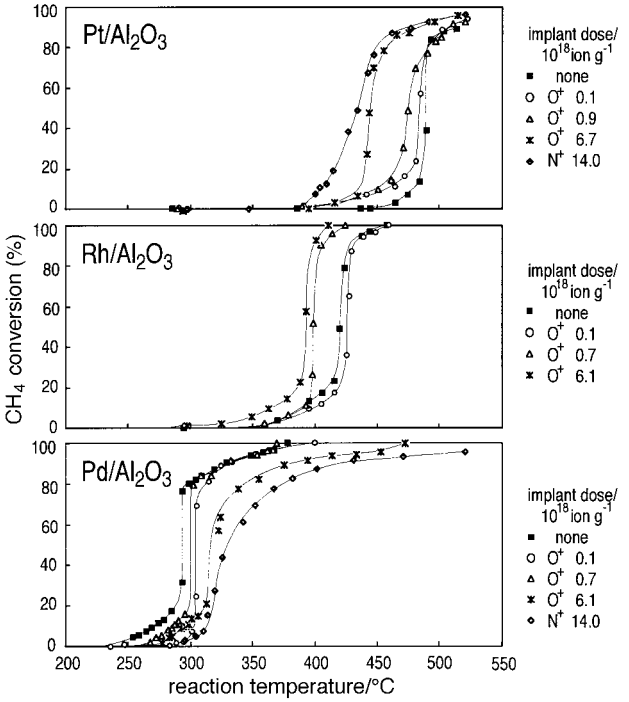

Fig. 2 Effect of O^+ and N^+ ion implantation on methane oxidation over 1 mass%Pt, Rh and Pd/Al_2O_3 catalysts. Reaction condition; CH_4 2 vol%, air 98 vol%, $W/F = 0.002$ (g cat) min cm^{-3}.

The higher implant dose caused a more serious levelling off effect on the methane oxidation over Pd/Al_2O_3 catalysts.

Surface analysis, crystal structure, and microstructure

To elucidate the effect of ion implantation on the methane combustion activity of supported Pt, Pd, and Rh catalysts, we have examined several characterizations by means of XPS, XRD, TEM and gas adsorption measurements. Fig. 3 shows the XPS spectra of Pd 3d and Rh 3d before and after ion implantation. A Pt 4f spectrum could not be detected because of overlapping with a strong Al 2p signal. For the as-prepared catalysts after calcination at 500 °C, the E_B of Pd $3d_{5/2}$ (336 eV) implied that almost all surface palladium species should be PdO. This is consistent with the fact that, in air at atmospheric pressure, the thermodynamically stable phase is PdO at temperatures below 780 °C, whereas metallic Pd is stable above 780 °C.[11–13] The XPS spectra of the implanted catalyst demonstrated that the Pd 3d signals shifted to lower binding energies with increasing O^+ dose. After implanting O^+ of 7.5×10^{18} ion g^{-1}, the Pd $3d_{5/2}$ spectrum consisted almost solely of a single peak at 334 eV, which represents the presence of only

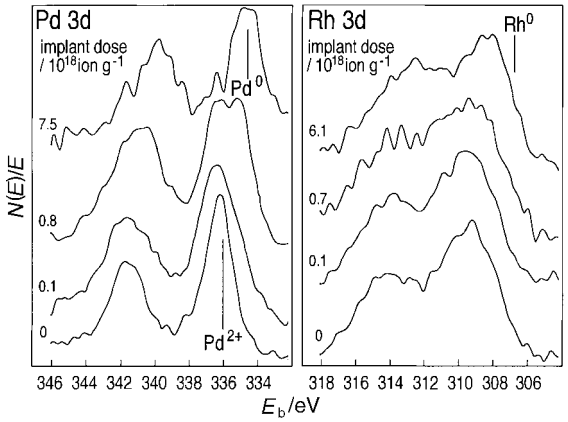

Fig. 3 Effect of O^+ implantation on XPS spectra of 1 mass%Rh/Al_2O_3 and 1 mass%Pd/Al_2O_3 catalysts

metallic Pd on the surface. Since an identical result was obtained after implanting N^+ of 14.0×10^{18} ion g^{-1}, the irradiation-induced reduction of PdO to Pd metal seems to be independent of the implanted ions. This is not a thermal dissociation process because the catalyst temperature during ion implantation was less than 300 °C. The phase transformation of the Pd catalyst was also observed by XRD measurements [Fig. 4(*a*)]. The as-prepared sample showed only the broad reflections of γ-Al_2O_3, but those from PdO were too weak to be observed because of the small loading amount and low crystallinity. The diffraction pattern was drastically changed after O^+ implantation of 7.5×10^{18} ion g^{-1}, which shows sharp reflections due to Pd metal. Thus, the irradiation-induced reduction is not limited to near-surface sites, but also penetrated to the bulk of supported noble metal particles. Interestingly, this sample also contained a small amount of α-Al_2O_3, which transformed from the γ-phase during the bombardment.

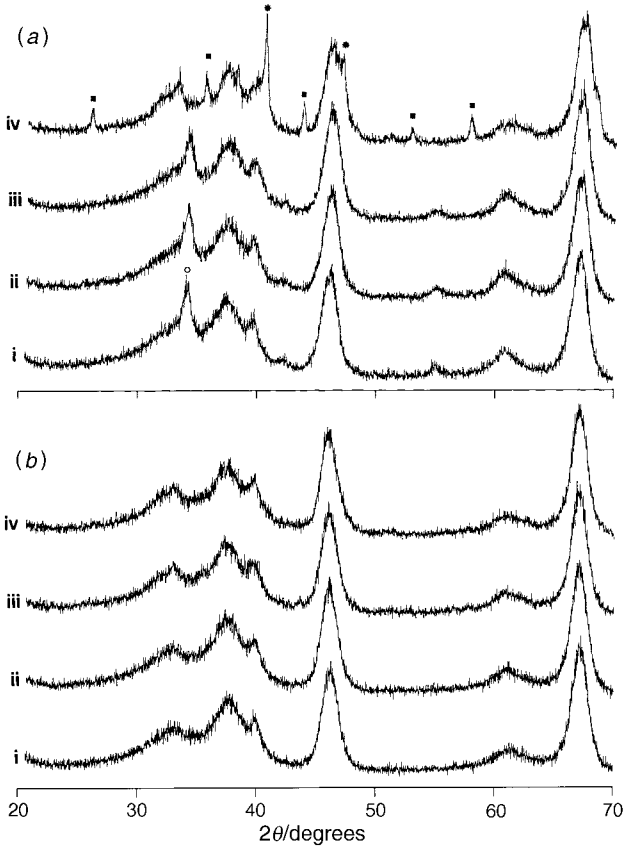

Fig. 4 Effect of O^+ implantation on powder XRD profiles of (*a*) 1 mass%Pd/Al_2O_3 and (*b*) 1 mass%Rh/Al_2O_3 catalysts. Implant dose: (*a*) i, none; ii, 0.1×10^{18}; iii, 0.8×10^{18}; iv, 7.5×10^{18} ion g^{-1}, (*b*) i none; ii, 0.1×10^{18}; iii, 0.7×10^{18}; iv, 6.1×10^{18} ion g^{-1}. Broad diffraction peaks without assignment are from γ-Al_2O_3 support; (*) Pd, (○) PdO, (■) α-Al_2O_3.

In case of the Rh/Al_2O_3 catalyst (Fig. 3), the as-prepared sample contained rhodium oxide as judged from the E_B of Rh $3d_{5/2}$ (310 eV) which is supposedly higher than that of Rh metal (307 eV). Although the signal gradually shifted to lower binding energies with increasing implant dose, Rh metal was not produced even after O^+ implantation of 6.1×10^{18} ion g^{-1}. In addition, very little change of crystal structure was detected by XRD measurement [Fig. 4(*b*)]. According to the thermogravimetric results of Newkirk and McKee,[14] heating hydrated $RhCl_3$ in air produces anhydrous $RhCl_3$ at <500 °C, Rh_2O_3 at <1040 °C, and finally Rh metal above 1040 °C. Thus, the effect of ion implantation on the oxidation state of Rh catalysts may be predicted from these dissociation temperatures which are much higher than that of PdO. This is reflected by the standard enthalpy of oxide formation, -82 kcal mol^{-1} for Rh_2O_3, whereas -20.4 kcal mol^{-1} is found for PdO.[15]

Ion implantation is also expected to change the particle size and microstructure of these noble metals, as well as the alumina support. The effect of ion implantation on the BET surface areas of the catalysts is shown in Fig. 5. In all cases, the surface area tends to decrease with an increase of implant dose. The most prominent change was observed for Pd/Al_2O_3, the surface area of which decreased from 191 m^2 g^{-1} to 150 m^2 g^{-1} after O^+ implantation of 7.5×10^{18} ion g^{-1}. This is in accord with the partial phase transformation of γ-Al_2O_3 to the α phase as is shown in Fig. 4(*a*). Similar but more significant surface area loss accompanied by a phase transformation was observed for γ-Al_2O_3 after certain amounts of Si^+ or B^+ implantation. The initial surface area (186 m^2 g^{-1}) in this case decreased to 98 m^2 g^{-1} (Si^+) or to 92 m^2 g^{-1} (B^+) for implant dose of 6.2×10^{18} ion g^{-1}.

We also conducted TEM observation of ion-implanted catalysts, but microstructural changes were not obvious for samples other than Pd/Al_2O_3. As shown in Fig. 6, as-prepared Pd/Al_2O_3 containing PdO particles of less than 10 nm were well dispersed on the fine Al_2O_3 powder matrix. After O^+ implantation of 7.5×10^{18} ion g^{-1}, however, a large number of crystalline grains (10–20 nm) consisting of only Pd were precipitated. From the XRD results shown in Fig. 4, these crystallites must be composed of Pd metal, which was produced by the decomposition of PdO. This means that irradiation-induced decomposition of PdO brought about significant grain growth

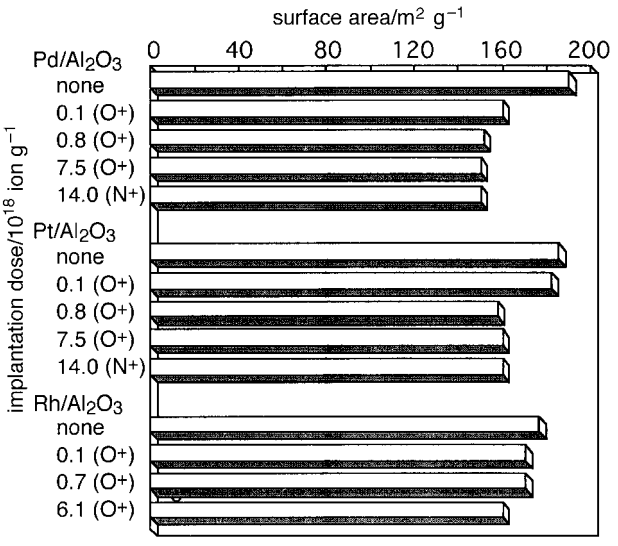

Fig. 5 Effect of O^+ and N^+ ion implantation on BET surface area of 1 mass%Pt, Rh and Pd/Al_2O_3 catalysts

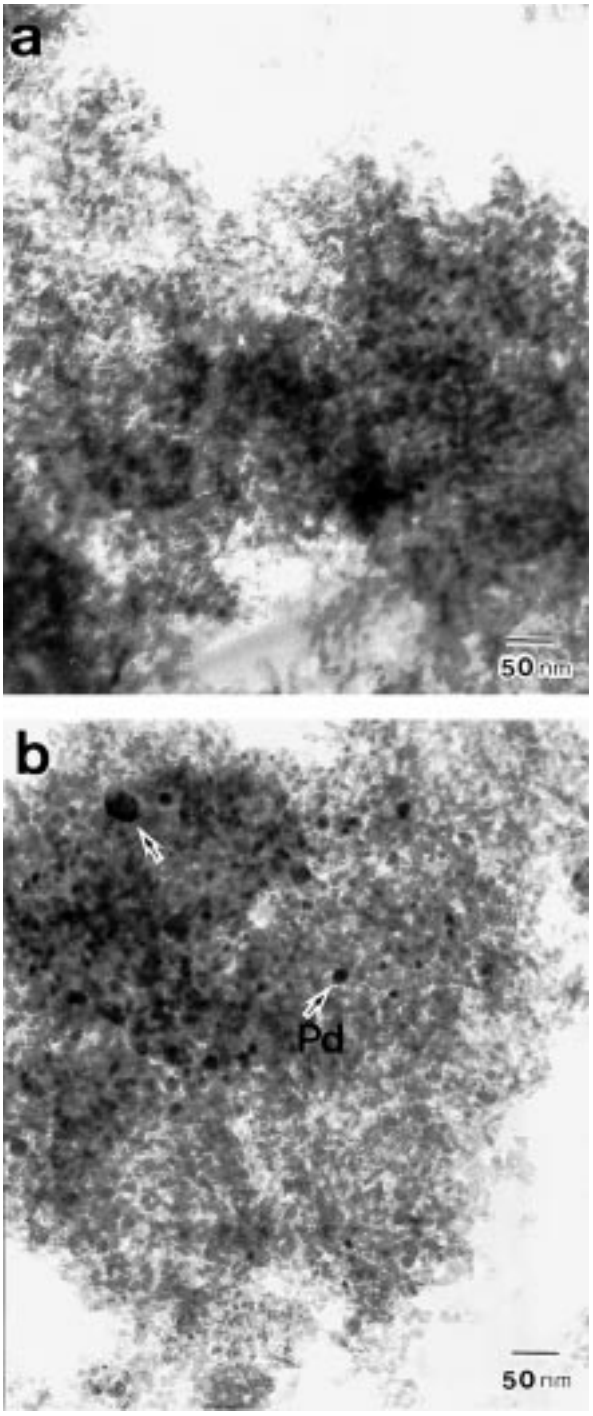

Fig. 6 TEM photograph 1 mass%Pd/Al_2O_3 (a) as prepared (after calcination at 500 °C) and (b) after O^+ implantation (implant dose 7.5×10^{18} ion g^{-1})

of Pd particles. We also observed several large grains of α-Al_2O_3, which were totally absent in as-prepared Pd/Al_2O_3. Precipitation of large grains of α-Al_2O_3 was also detected in Pt- and Rh-supported catalysts by means of selected area electron diffraction. However, it seems that their number is too small to be observed by powder XRD diffraction measurements.

Since the microstructural changes of Pt and/or Rh after ion implantation were invisible to TEM, we also conducted preliminary measurements of the hydrogen chemisorption isotherms at room temperature (Table 1). Apparently, the O^+-implanted sample consists of platinum particles with higher dispersion on alumina support. This is considered one important reason to enhance the methane combustion activity of these catalysts.

Table 1 Effect of O^+ ion implantation on dispersion of platinum for 1 mass%Pt/Al_2O_3 catalyst

implant dose/ion g^{-1}	dispersion (%)
(as-prepared)	38
0.1×10^{18}	62

Effect of ion implantation on catalytic properties

As was described above, the ion implantation of 100 keV O^+ and/or N^+ enhanced the methane combustion activity of Pt or Rh/Al_2O_3, but deactivated the Pd catalyst. These effects appear to originate from alteration of the oxidation state as well as dispersion of supported noble metals. The metallization of oxides by the loss of anions during ion bombardment has been reported for many systems.[16] Losing certain atoms from a solid as a result of beam–surface interactions can be classified as collisional, thermal, or electronic sputtering. A large number of examples have been recognized as electronic sputtering processes, which occur with incident ions, electrons, or photons having the electronic stopping power, (dE/dx) (E = energy of incident ions, x = depth beneath the surface), which would be enough to break bonds on each atomic layer.[16] These particles incident on the oxide solid cause the following ionization of lattice oxygens, *i.e.*, the loss of bonding:

$$O^{2-} = O^- + e^-;\ O^- = O^0 + e^-$$

or corresponding processes involving holes or the formation of antibonding states. If these less negatively charged oxygen species are formed on the surface of noble metals as well as Al_2O_3, they may take part in catalysis. For instance, O^- species over metal oxide catalysts are well known to activate methane at $\geqslant 400$ °C.[17] For the catalysts used in this study, however, the presence of oxygen species other than O^{2-} was not detected in the O 1s XPS measurements. We have also tried catalytic CH_4 combustion over γ-Al_2O_3 alone. The result showed that the temperature dependence of CH_4 conversion was not affected by the ion implantation. The loss of bonding in the ion implantation process would lead to thermal release and the formation of antibonding states would give a more violent expulsion. Besides this type of direct interaction, sputtering of oxide ions may be brought about by interatomic Auger decay or diffusing defects,[16] but the detailed mechanism of electronic sputtering has not been solved at this stage.

When the irradiation-induced metallization proceeds inside PdO particles, activated atomic diffusion will lead to significant grain growth of Pd metal. On the other hand, the reason for the increased catalytic activity of implanted Pt and Rh catalysts is not clear at this stage. One plausible explanation is based on improved dispersion of these metals as a result of the ion implantation. As was observed for Pt catalysts (Table 1), under the irradiation, these metals may tend to increase their surface area without decreasing their particle size. This implies that topographic change causes surface roughness to increase the net surface area. Further characterization was carried out for particle size, morphology and surface roughness of noble metal particles to clarify this point.

As evident from from Fig. 4, high dose implantation also resulted in the transformation of γ- to α-Al_2O_3. It is well known that this phase transformation usually requires heating above 1000 °C, which is much higher than temperatures (<300 °C) of the sample under ion beam irradiation. Thus, the present result is attributable to the ion beam–solid interactions as in the case of irradiation-induced dissociation of PdO. The penetration depth of O^+ or N^+ ions accelerated at 100 keV is considerably larger than the mean particle size of γ-Al_2O_3.

This should cause a large number of point defects through collision cascades and activated atomic diffusion inside γ-Al_2O_3 particles even at low temperatures. Similar irradiation-induced recrystallization has been reported for amorphous alumina films deposited on a sapphire substrate.[18] In this case, the regrowth proceeds through two distinct steps; the entire amorphous layer first crystallizes into γ-Al_2O_3 with poor crystallinity, followed by a second transformation into α-Al_2O_3, which shows good epitaxial quality. The γ to α phase transformation of Al_2O_3 powders is known to be accompanied by drastic surface area loss.[19] In the same manner, the BET surface areas of irradiated catalysts decreased at higher implant doses (Fig. 5), with the simultaneous deposition of large α-Al_2O_3 grains.

Conclusions

The present study has revealed that ion implantation significantly influenced the catalytic activity of supported Pd, Pt, and Rh catalysts for methane combustion. The effect was strongly associated with the reduction and the surface area of noble metal species. Ion implantation deactivated Pd/Al_2O_3 catalysts as a result of the dissociation of PdO and simultaneous grain growth of Pd metal. In contrast, the methane combustion activity of Rh/Al_2O_3 and Pt/Al_2O_3 was enhanced by ion implantation, probably due to the increased surface areas of these noble metals.

Ion implantation experiments of this study were carried out as a part of the research project of the Petroleum Energy Center commissioned by the New Energy and Industrial Development Organization in 1994.

References

1 K. W. Mayer and S. S. Lau, in *Surface Modification and Alloys*, ed. J. M. Poate, G. Foti and D. C. Jacobson, Plenum Press, New York, 1983, p. 241.
2 *Ion Bombardment Modification of Surfaces*, ed. O. Anciello and R. Kelly, Elsevier, Amsterdam, 1984.
3 K. Kohlhof, *Nucl. Instrum. Methods B*, 1995, **99**, 662.
4 A. M. Ektessabi, *Nucl. Instrum. Methods B*, 1995, **99**, 610.
5 A. Charlesby, *Nucl. Instrum. Methods B*, 1995, **105**, 219.
6 J. M. Martin, D. D. Cohen, G. J.Russell, N. Dytlewski and D. J. Evans, *Nucl. Instrum. Methods B*, 1995, **106**, 618.
7 R. Prasad, L. A. Kennedy and E. Ruckenstein, *Catal. Rev.*, 1984, **26**, 1.
8 J. G. Firth and H. B. Holland, *Trans. Faraday Soc.*, 1969, **65**, 1121.
9 Y.-F. Yu Yao, *Ind. Eng. Chem. Prod. Res. Dev.*, 1980, **19**, 293.
10 S. H. Oh, P. C. Mitchell and R. M. Sieewert, *J. Catal.*, 1991, **132**, 287.
11 C. Mallika, O. M. Sreedharan and J. B. Gnanamoorthy, *J. Less-Common Met.*, 1983, **95**, 213.
12 K. Sekizawa, M. Machida, K. Eguchi and H. Arai, *J. Catal.*, 1993, **142**, 655.
13 J. R. Anderson, in *Structure of Metallic Catalysts*, Academic Press, New York, 1975, p. 199.
14 A. M. Newkirk and D. W. McKee, *J. Catal.*, 1968, **11**, 370.
15 *CRC Handbook of Chemistry and Physics*, ed. R. C. Weast, CRC Press, Boca Raton, FL, 72nd edn., 1991.
16 R. Kelly, in *Ion Bombardment Modification of Surfaces*, ed. O. Anciello and R. Kelly, Elsevier, Amsterdam, 1984, p. 25.
17 C. Yu, W. Li, W. Feng, A. Qi and Y. Chen, *Proc. 10th Int. Congress on Catal.*, Elsevier, Amsterdam, 1993, p.1119.
18 N. Yu and M. Nastasi, *Nucl. Instrum. Methods. B*, 1995, **106**, 579.
19 H. Arai and M. Machida, *Appl. Catal. A*, 1996, **138**, 161.

Paper 7/06503E; *Received* 5*th September*, 1997